Available online at www.sciencedirect.com
SCIENCE DIRECT
Polymer 46 (2005) 5966–5978
polymer
www.elsevier.com/locate/polymer

Influence of temperature-induced coalescence effects on co-continuous morphology in poly(ε-caprolactone)/polystyrene blends

Pierre Sarazin, Basil D. Favis*

CREPEC, Department of Chemical Engineering, Ecole Polytechnique de Montreal, 2900 Edouard Montpetit, P.O. Box 6079, Station Centre-Ville, Montréal, Que., Canada H3C 3A7

Received 30 September 2004; received in revised form 8 October 2004; accepted 20 April 2005
Available online 16 June 2005

Abstract

This paper demonstrates that temperature-induced coalescence effects during melt mixing have a major influence on the concentration range of dual-phase continuity and an order of magnitude effect on the co-continuous microstructure phase size. A detailed study on the effect of temperature of blending on the morphology of immiscible poly(ε-caprolactone)/polystyrene blends is presented. Polycaprolactone (PCL) and polystyrene (PS) are blended in a batch mixer at 50 and 5 min for various temperatures. The continuity of the phases is obtained by selective extraction of each phase and the microstructure is analyzed using image analysis on SEM micrographs and mercury intrusion porosimetry. It is observed that the blending temperature has only a small effect on the morphology up to a PS or PCL composition of about 20 or 30%. However, beyond that composition the effect is dramatic. The microstructure of the 50/50 blend demonstrates a phase size (d_v) of 8.5 μm at 230 °C and 1.1 μm at 155 °C. Furthermore, the concentration range of co-continuity is broadened from 50–65%PS at 230 °C to 30–70%PS at 155 °C. The results at lower concentrations indicate that the temperature has little effect on the overall deformation/disintegration process, which appears to be due to compensating effects. For example, for PS in PCL, shear stress increases significantly at lower temperatures, but is counterbalanced by an increase in the viscosity ratio, elasticity of the phases and an increase in interfacial tension. Beyond a volume fraction of 0.30, the effect of temperature on coalescence plays a dominant role on the final morphology. It is shown in this paper that the observed morphology effects are controlled by the merging stage of coalescence. The data indicate the significant potential of mixing temperature as a tool for the morphology control of co-continuous polymer blends.

Keywords: Coalescence phenomena; Immiscible binary blends; Co-continuous morphology

1. Introduction

The development of new multiphase polymer blend materials is mainly dependent on the control of the interfacial chemistry and the control of the microstructure. In a binary immiscible polymer blend, at low concentration of the dispersed phase, the microstructure is characterized by a dispersed droplet/matrix type morphology [1]. Increasing the concentration of the minor phase leads to the co-continuity region where both phases are fully continuous in the bulk for a certain range of compositions. At higher concentrations phase inversion leads once again to the dispersed phase/matrix morphology. Recently, there has been significant interest in polymer blends with co-continuous morphology [2,3]. Due to their interconnected nature, co-continuous morphologies have the potential to significantly widen the application range for polymer blends [4–6]. They can offer specific advantages for cases where phase percolation is an important consideration.

Li et al. [7] examined the role of the interface on the formation of the co-continuous structure for three categories of immiscible blends interface based on HDPE, PS, SEBS and SEB components. Using the technique of solvent extraction of the dispersed phase, the limits of the co-continuity of the extracted phase was defined by the region for which the continuity of the extracted phase becomes higher than 90–95% and remains nearly constant until the point of the disintegration, i.e. the composition at which the mechanical integrity of the extracted blend cannot be assured. The size of the extracted phase was assessed by the

* Corresponding author. Tel.: +1 514 340 4711x4527; fax: +1 514 340 4159.
E-mail address: basil.favis@polymtl.ca (B.D. Favis).

0032-3861/$ - see front matter © 2005 Elsevier Ltd. All rights reserved.
doi:10.1016/j.polymer.2005.04.064

pore size of the porous structure as obtained using the BET technique. The type I interface was defined as that for compatible binary blends (i.e. HDPE blended with one of its copolymers), the type II corresponded to the interface of the incompatible binary blends (HDPE/PS system), and the type III to the interface of the compatibilized ternary systems (i.e. HDPE/PS system compatibilized by copolymers). Type II systems demonstrated a strong dependence of scale with composition while the type I and III interfaces possessed co-continuous microstructures where the phase size was virtually independent of composition. The interface type also had a strong influence on the breadth of the apparent region of co-continuity with the widest range attributed to the type I and the narrowest to the type III. Using arguments based on thread lifetime vs. droplet lifetime during melt processing, Li et al. [7] proposed a conceptual mechanism for the effect of the interface on co-continuity formation that effectively explains all of their various experimental observations. For the type II system with high interfacial tension, the continuity development and microstructural features are consistent with a mechanism dominated by droplet–droplet coalescence (droplet lifetime > thread lifetime).

For two particles of dispersed phase to coalesce, they must first come into close proximity of each other by the flow driven shear or extensional field. The coalescence phenomena for two droplets is mainly described as a four step mechanism: the collision between the two particles, the drainage of the matrix film between colliding droplets, the rupture of the matrix film and the final merging into a fully coalesced larger spherical particle [8,9]. Experimental studies on flow-induced coalescence in polymer blends are relatively recent and interesting work has been carried out by Vinckier et al. [10] and Lyu et al. [11,12].

To date very little work has been carried out on the influence of temperature on co-continuous morphology generation in immiscible polymer blends [13–15]. The influence of temperature on the morphology of polymer blends is a complex package of fluid dynamics since it results in order of magnitude effects on the rheology of the components which, in turn, affects the deformation/disintegration processes, coalescence and capillary breakup phenomena. The objective of this work is to carry out a detailed morphology analysis of the influence of the mixing temperature on co-continuity development for type II incompatible binary blends comprised of poly(ε-caprolactone)/polystyrene. The PCL/PS polymer system is used since each component can be selectively dissolved allowing for a complete study of the co-continuous region. These components are also stable over a large range of temperatures and times of mixing.

2. Experimental procedure

2.1. Materials

A polystyrene from Dow (PS), and a poly(ε-caprolactone) from Solvay-Interox (PCL) were used. Some of the characteristics of the resins used are reported in Table 1. The densities of the polymers at various temperatures were needed in order to mix the polymers on a volume fraction basis.

The densities at room temperature were measured via a hydrostatic balance, using the weight of a polymer sample in air and in ethanol.

$$\rho = \frac{W_{\text{air}}}{W_{\text{air}} - W_{\text{ethanol}}} \rho_{\text{ethanol}} \quad (1)$$

where ρ is the density of the polymer, ρ_{ethanol} is the density of ethanol at test temperature, W_{air} and W_{ethanol} are the weight of the polymer specimen measured in air and in ethanol, respectively. Three specimens of each polymer were used.

The densities in the melt state were determined via dilatometry using a fully automated Gnomix PVT (pressure–volume–temperature) high-pressure dilatometer (heating at 2.5 °C/min). The densities at atmospheric pressure were fitted from data obtained at 100, 600 and 1200 bars.

2.2. Rheological analysis

Rheological characterization was carried out using a parallel-plate geometry rheometer AR2000 from TA Instruments, equipped with a controlled convection-radiant heating chamber (ETC). The disk-shaped samples used were compression molded at 140 and 200 °C for PCL and PS, respectively. An oscillation mode at a frequency of 0.01 rad/s was used to study the stability of the raw materials at testing temperatures. Stress sweeps were performed to define the region of linear viscoelasticity. The experiments were then performed in the dynamic mode at 140, 155, 170, 185, 200, 210, and 230 °C in the range of 0.01–150 rad/s, under a nitrogen atmosphere. Steady shear

Table 1
Characteristic properties of materials

	M_w	M_n	Density at 20 °C (g/cm^3)	Glass temperature (°C)	Melting point (°C)	Supplier
PCL	120,000	69,000	1.14	−60	60–62	Solvay Interox
PS	192,000	–	1.04	100–105		Dow

flow tests were also carried out at 140, 170 and 200 °C. It was possible to measure the shear viscosities from 0.01 s^{-1}. The normal force needed to be higher than 0.1 N to be measured. Loss of viscosity and normal force values appeared around 1–2 s^{-1}, due to the onset of the expulsion of the specimen out of the parallel plate. The difference between the primary and secondary normal stress difference $N_1(\dot{\gamma}) - N_2(\dot{\gamma})$ was obtained by steady shear flow measurements using concentric disk geometry. Other than the stability and stress sweep tests, all experiments were carried out at least in duplicate.

2.3. Blend preparation

Binary blends of polystyrene and polycaprolactone were prepared by melt mixing under a flow of dry nitrogen in a Haake Rheomix 600 batch mixer equipped with a Haake System 90, operating at 50 rpm. Using the technique described by Bousmina et al. [16], the average shear rate in the mixer was estimated to be about 25 s^{-1}. The mixing temperatures were 230, 200, 170 and 140 °C. Based on the densities at mixing temperature, the mass of material charged into the mixer was chosen so that a constant volume of 50 cm^3 was achieved for each sample. The mixing torque data and the temperature in the melt of the blends were collected during the blending process. After feeding the components, the blends were mixed for 5 min. After the specified time of mixing, the roller blades were stopped, the chamber was opened and the blends, while still blown by the cold nitrogen gas, were rapidly pulled out from the chamber and quenched in liquid nitrogen to freeze-in the morphology. All the blend concentrations are reported as volume fraction. The maximum error for the weight of materials was measured as $\pm 0.1\%$.

Various times of mixing were evaluated to select the time to reach a steady-state initial morphology. At 140 °C, tests for PS/PCL 10/90 and 50/50 done at 4, 5, and 10 min of mixing did not indicate a change of morphology and pore size. However, at this set temperature, the torque decreases slightly with mixing time.

Care needs to be taken to remove the sample from the mixer because the entire mixer cannot be frozen after the required mixing time. Post-mixing quiescent annealing is thus likely to appear, and this effect is expected to be more dramatic at high temperatures of mixing. As mentioned, among others, by Guo et al. [17], the coalescence rate can be very fast, especially in the early stages of quiescent annealing. Such a post mixing coarsening will depend more heavily on the matrix viscosity and the effect will be more pronounced at compositions rich in the low viscous phase [18] (i.e. for PS dispersed in PCL). As considered by Janssen and Meijer [9], the quenching procedure may largely influence the final morphology. Less than 15 s was needed to access the mixing chamber. In less than 1 min, all the material in the mixing chamber was removed and quenched in liquid nitrogen. The time for which the blend remains at the mixing temperature in the mixer is assumed to be about 30 s, but some minor annealing at high mixing temperature is unavoidable.

2.4. Solvent extraction and continuity of PS and PCL phases

Extractions were performed in bottles at room temperature. Cyclohexane and acetic acid were used to extract PS and PCL, respectively. The specimens were then dried in a vacuum oven. The extraction time for each composition was determined as the time at which the weight of the specimens did not change after drying. Shorter times for extraction and drying were found for compositions with high continuity of the removed phase. Shorter times for extraction were also found when the size of the extracted phase is greater. A gravimetric method was used to calculate the extent of continuity of the PS and PCL phase using this simple equation

$$\%\ \text{Continuity of } P = \left(\frac{\text{Weight } P_{\text{initial}} - \text{Weight } P_{\text{final}}}{\text{Weight } P_{\text{initial}}}\right) \times 100\% \quad (2)$$

where P corresponds to the removed phase.

Ten specimens of various weights and shapes were used for each blend composition. The standard deviation was found to be less than 0.5 in the co-continuous region and around 2 at low concentration of the dispersed phase. However, at intermediate concentrations of dispersed phase, the standard deviation can reach as high as 7. At these concentrations, small variations of blend composition can significantly modify the continuity percent of the extracted dispersed phase.

Dissolution of the matrix (PS with cyclohexane and PCL with acetic acid) was also performed to observe the shape of the dispersed phase. It was ensured that the dispersed PS phase, glassy at room temperature, retained its shape after dissolution of the matrix. When the PCL is the dispersed phase, agglomerates are formed after the matrix dissolution, and a number of methods to attempt to separate them were unsuccessful. Thus, only tests after PCL matrix dissolution gave interpretable results.

2.5. Microtomy and scanning electron microscopy (SEM)

The specimens were microtomed to create a perfect plane face using a Reichert Jung 2050 Supercut Microtome with a glass knife and equipped with the Liquid Nitrogen Freezing Device LN20. After selective solvent extraction and coating with a gold–palladium alloy, the microtomed specimens were observed under a Jeol JSM 840 scanning electron microscope at a voltage of 5 or 10 kV. The PS dispersed phase after matrix dissolution was also observed by SEM.

2.6. Image analysis and mercury porosimetry

A semi-automatic image analysis technique using a Wacom digitalization table and SigmaScan Pro software was used to measure the diameters of the dispersed phase for the matrix/dispersed phase morphology type. SEM micrographs were analyzed for each sample to estimate the number average diameter, d_n, and volume average diameter, d_v. Since the microtome does not necessarily cut the dispersed phase at the equator and since it is necessary to correct for the dispersity, a correction factor [19] was applied to the diameters determined from the SEM micrographs. About 200–500 diameters were measured per sample. For a fixed magnification, the maximum error for the average diameter measurements was about $\pm 10\%$.

The porosity of 50/50 blend specimens was estimated by mercury intrusion porosimetry using a Micromeritics Poresizer 9320. The experimental data treatment is based on the Washburn equation [20,21]

$$P = -\frac{2\sigma \cos\theta}{r} \tag{3}$$

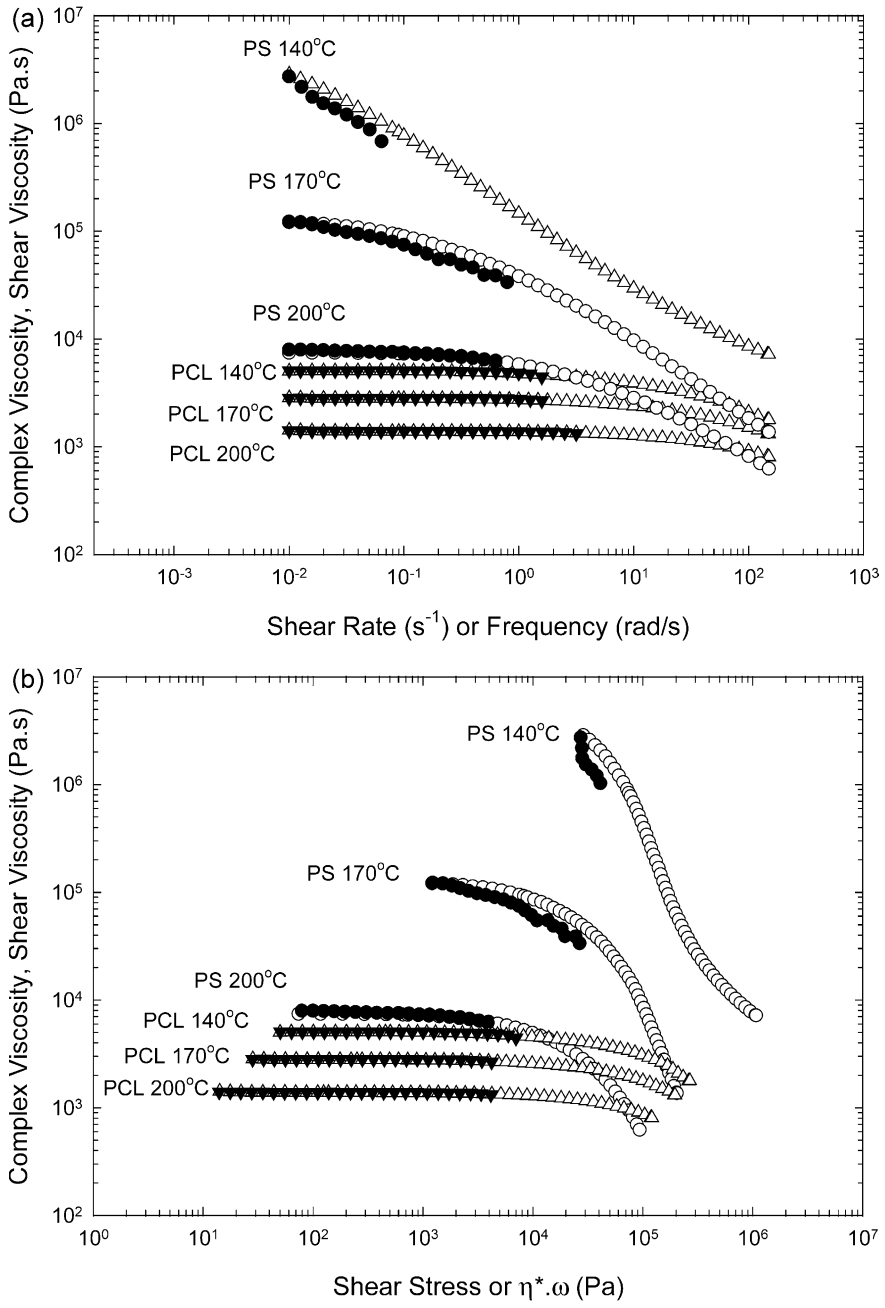

Fig. 1. (a) Viscosity as a function of shear rate or frequency, for three temperatures. (b) Viscosity as a function of shear stress or estimated shear stress ($\eta^*\omega$) for three temperatures (white symbols: dynamic measurements, black symbols: steady shear flow measurements).

where P is the applied pressure, r is the radius of the pore, σ is the surface tension of the mercury and θ is the contact angle between polymer and mercury (480 mN/m and 140°, respectively were used for all measurements). This method can provide the number-average diameter (by the volume/surface ratio), the volume-average diameter, and the pore size distribution.

3. Results and discussion

3.1. Rheology data and comments on the experimental methods

In order to relate the rheological functions measured by a

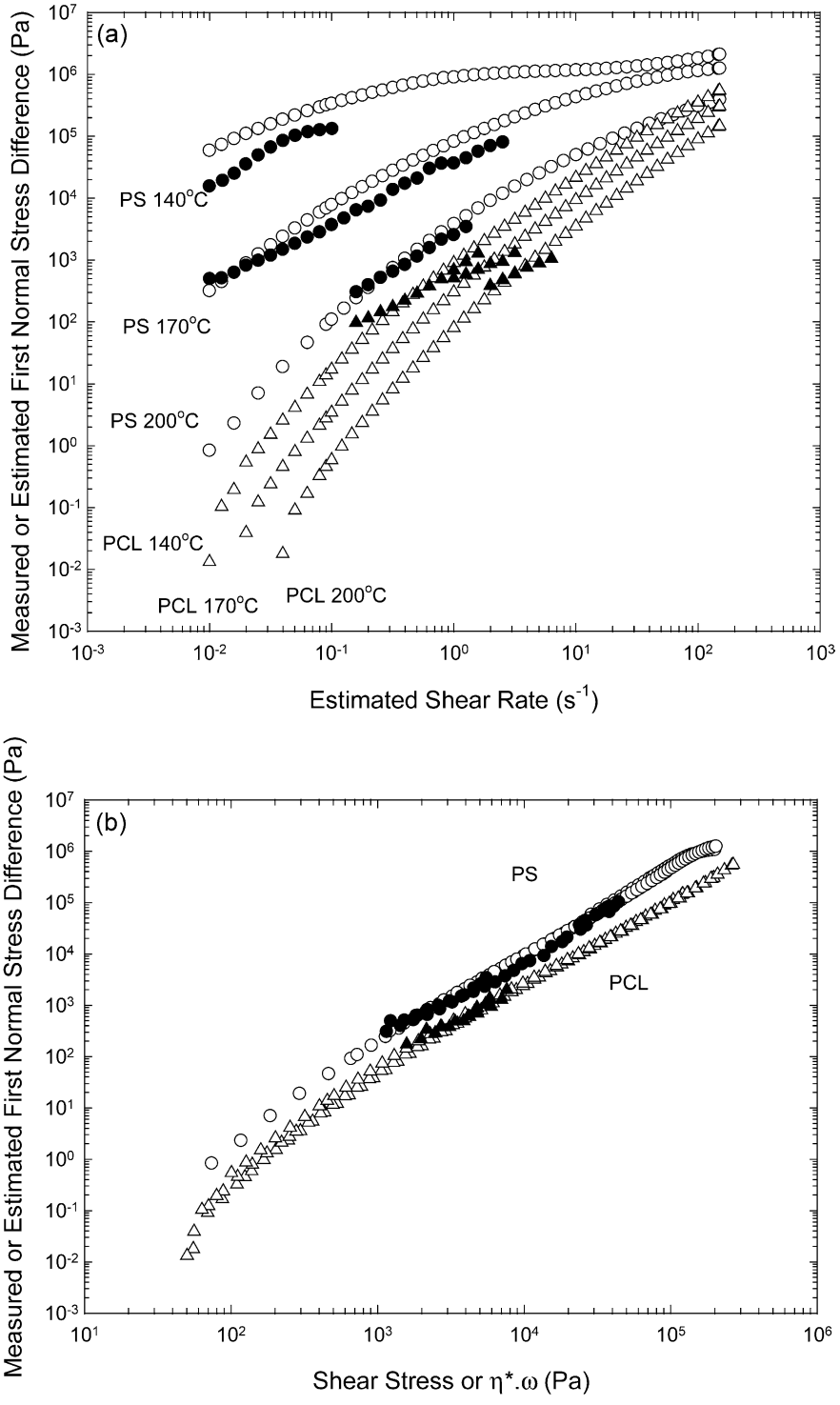

Fig. 2. (a) Measured or estimated first normal stress difference as a function of the shear rate for three temperatures. (b) Measured or estimated first normal stress difference as a function of the shear stress or estimated shear stress ($\eta^*\omega$) for three temperatures (white symbols: estimated from dynamic measurements, black symbols: measured from steady shear flow measurements).

rheometer with a melt mixing operation, we verified: (i) the relation between the rotor speed value and the shear rate; (ii) the validity of the Cox-Merz relation and Laun relation used and (iii) the use of similar temperatures in the rheological data and during mixing. We also compared the viscoelastic properties of the blend components, taking the shear stress of the matrix or the shear rate as reference.

The Cox-Merz relation [22] was found to be valid for our polymers as illustrated by Fig. 1(a), with some difference at 140 °C for PS. Since the pure materials follow the Cox-Merz relation, the shear stress is estimated as the product of the angular frequency and the measured complex viscosity. Fig. 1(b) shows the viscosity for the raw materials used as a function of shear stress or estimated shear stress.

The Laun empirical relation [23], which relates the steady-state primary normal stress coefficient in steady shear flow to the dynamic moduli, was applied to the dynamic data of the pure components.

$$\frac{N_1}{\dot{\gamma}^2} = \frac{2\eta''(\omega)}{\omega}\left[1+\left(\frac{\eta''}{\eta'}\right)^2\right]^{0.7} = 2\frac{G'}{\omega^2}\left[1+\left(\frac{G'}{G''}\right)^2\right]^{0.7} \quad \text{for } \omega = \dot{\gamma} \tag{4}$$

The difference between the normal stresses $N_1(\dot{\gamma}) - N_2(\dot{\gamma})$ was obtained by steady shear flow measurements using concentric disk geometry. N_2 was considered to be negligible compared to the primary normal difference. The primary normal stress difference from steady shear flow measurements and calculated by the Laun relation are plotted as functions of estimated shear rate and shear stress in Fig. 2. The relation was found to be valid for the range of shear rate experimentally used.

During mixing, we observed that the melt temperature can reach a temperature plateau higher than the set temperature even if the temperature in the heating plates was well controlled. Table 2 indicates the variation between the set temperature and the average temperature in the melt after 5 min of mixing. At 230 °C, there was no difference between the set and measured temperatures. This variation of temperature increases when the temperature of mixing decreases. Taking notice of these temperature variations, the rheological data were also measured at temperatures close to the average melt temperature measured in the mixer after 5 min of mixing. We found an accurate correlation for pure components when we compare the viscosities measured at 25 rad/s at these new temperatures with those calculated from the torque data. Thus the rheological data of the pure components presented in Tables 3 and 4 are taken at 230, 210, 185 and 155 °C. The ratios in Table 4, corresponding to the ratios of the rheological functions for the pure components, are indicated since this is the typical parameter used in immiscible polymer blends to predict the position of the phase inversion. The viscosity of PS was found to be higher than that of PCL except at 230 °C, while $N_{1,PS}$ was always higher than $N_{1,PCL}$. From 230 to 155 °C, the PS viscosity at 25 rad/s increased by 10 times, while the PCL viscosity tripled. The viscosity ratio η^*_{PS}/η^*_{PCL} at constant shear rate and constant shear stress increases from 0.8 to 2.8 and 0.6 to 42.3, respectively. The difference between $N_{1,PS}$ and $N_{1,PCL}$, taken at constant shear stress increases when the temperature decreases (Table 5).

3.2. Effect of temperature on morphology at 5% dispersed phase

The minor phase morphology demonstrates little effect of temperature at 5% of dispersed phase, as shown in Figs. 3 and 4 for 155 and 230 °C. The morphology of the PS phase after dissolution of the matrix consists of droplets for all the mixing temperature (Fig. 5), clearly establishing that no stable thread was formed. However, the PCL in PS matrix could not be analyzed by matrix dissolution. For 5%PCL the phase size is found to be 0.11 and 0.14 μm (d_v) at 155 and 230 °C, respectively. Despite the order of magnitude differences in the viscosity and elasticity of the systems, virtually no difference is observed in the final morphology. A thorough examination of the rheological properties of the system in Tables 3 and 4 appear to indicate that this result is due to compensating effects in the system. From 230 to 155 °C, the PS shear stress increases significantly from 16 to 178 kPa, but is counterbalanced by an increase in the elasticity of the phases (first normal stress coefficient of PS increases from 21.7 kPa to 1.1 MPa and that for PCL increases from 7.3 to 48.2 kPa). Biresaw and Carriere [24] found that the interfacial tension was 7.6 ± 1.8 mN/m for the PCL/PS system and considered that, within experimental error, it remained constant for the range of their measurements (160, 180 and 200 °C). It is well known however, that the interfacial tension increases with decreasing temperature and that this effect can be particularly pronounced for large molecular weight distributions [25,26]. Since

Table 2
Internal mixer data

Blending conditions	Fixed heating temperature (°C)	Melt temperature measured in the mixer (°C)	Torque ratios T_{PS}/T_{PCL} at 50 rpm
1	230	229–231 (230)	0.74
2	200	209–211 (210)	1.05
3	170	180–185 (182)	1.68
4	140	153–160 (156)	2.72

Table 3
Viscosities and estimated shear stresses for pure PS and PCL samples, at 26.1 rad/s

T (°C)	$\eta^*_{PS} \times 10^{-3}$ (Pa s)	$\tau_{PS} = \omega\eta^*_{PS} \times 10^{-3}$ (Pa)	$\eta^*_{PCL} \times 10^{-3}$ (Pa s)	$\tau_{PCL} = \omega\eta^*_{PCL} \times 10^{-3}$ (Pa)
230	0.6	16	0.8	22
210	1.2	30	1.0	26
200	1.8	47	1.2	30
185	2.7	71	1.5	39
170	4.8	126	2.1	55
155	6.8	178	2.4	63
140	16.8	439	3.3	85

significantly increasing matrix shear stress should reduce the phase size and increasing dispersed phase elasticity and interfacial tension should increase phase size [27,28], the overall result from these compensating effects is very little effect on the overall deformation/disintegration processes during mixing and final phase size.

At 5% of dispersed phase, the size of the PS phase in the PCL matrix (PS in PCL) is twice that of PCL in the PS matrix (PCL in PS) at both 155 and 230 °C (Figs. 3 and 4). The same trend is found up to 20% of dispersed phase. These results can again be explained by an examination of the rheological properties of the system. Although the viscosity ratios for the PS/PCL and the PCL/PS system are close to unity, there are significant differences in the matrix shear stress and the

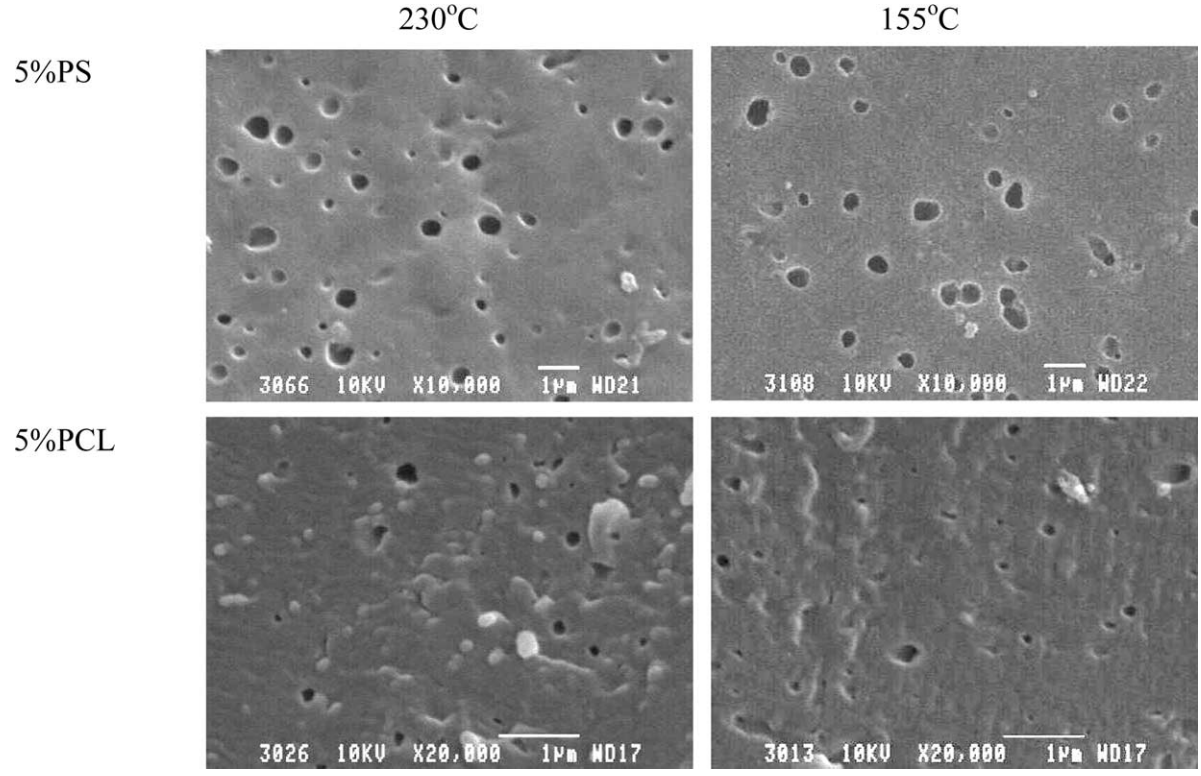

Fig. 3. Morphology of blends with dispersed phase volume fraction of 5%. The minor phase is extracted with a solvent. The white bar indicates 1 μm.

Table 4
Viscosity and elasticity ratios

T (°C)	η^*_{PCL}/η^*_{PS}	G'_{PCL}/G'_{PS}	$\tan\delta_{PCL}/\tan\delta_{PS}$ at 26.1 rad/s	$N_{1\,PCL}/N_{1\,PS}$ at 26.1 s^{-1}	η_{PCL}/η_{PS}	$N_{1\,PCL}/N_{1\,PS}$ at constant shear stress
PS matrix						
230	1.30	0.41	3.65	0.34	1.20	0.23 ± 0.02
210	0.85	0.26	4.22	0.18	0.84	
185	0.55	0.18	5.48	0.08	0.49	
155	0.35	0.14	5.87	0.04	0.23	
PCL matrix						
230	0.77	2.42	0.27	2.98	0.65	4.45 ± 0.24
210	1.17	3.80	0.24	5.51	1.33	
185	1.80	5.68	0.18	12.31	4.18	
155	2.82	7.35	0.17	22.89	42.31	

Table 5
N_1 difference as a function of the temperature and the matrix

Temperature (°C)	$N_1^{PS} - N_1^{PCL}$ at constant estimated shear rate ($\times 10^{-3}$ Pa)	$N_1^{PS} - N_1^{PCL}$ (PS matrix) at constant shear stress ($\times 10^{-3}$ Pa)	$N_1^{PS} - N_1^{PCL}$ (PCL matrix) at constant shear stress ($\times 10^{-3}$ Pa)
230	14.4	16.2	26.3
210	48.9	47.2	35.2
185	246.1	210.9	70.8
155	1054.3	826.0	178.6

elasticity ratios. The very high PS matrix shear stress as well as the very high PS/PCL elasticity ratio would be expected to result in a finer dispersed phase morphology for the PCL in PS system as observed here.

3.3. Effect of temperature on microstructure and continuity development at high concentration of dispersed phase

Beyond a concentration of 20% of dispersed phase, smaller phase sizes are observed for blends mixed at the lower temperature (Figs. 6–8). Furthermore, at 30% dispersed phase, the shape of the dispersed phase becomes highly dependent on the temperature of mixing. At that concentration and at 230 °C the dispersed phase is clearly spherical in nature while at 155 °C, the morphology resembles multiple coalescing droplets in the process of merging together (Fig. 6). This effect is even more clearly demonstrated in the matrix dissolution experiments shown in Fig. 7 for the 20 and 30% PS blends. At 230 °C the dispersed PS phase is clearly spherical in nature. At 155 °C multiple connected droplets can be seen in the process of merging together. Dramatic effects are observed for the 50/50 blends, as indicated in Figs. 4 and 9. At that concentration, the volume average diameters of the phase size are about 1.1 μm at 155 °C, 2.2 μm at 185 °C, 5.6 μm at 210 °C and 8.5 μm at 230 °C as measured by mercury intrusion porosimetry. It is interesting to note that, at a given temperature, the sizes of both phases are quite similar at 50% concentration.

Fig. 10 shows the percent continuity of PS and PCL as a function of blend composition obtained after solvent extraction. At 30%PS and at 155 °C, the PS phase is already fully continuous throughout the blend, i.e. the phases are co-continuous. It is found that the range of co-continuity greatly increases when the temperature of mixing decreases. This effect is observed for both the PS phase in a PCL matrix and also for the PCL phase in a PS matrix, but is much more pronounced for the former case.

Blends of PS dispersed in a PCL matrix are characterized by high interfacial tension (type II, as described by Li et al. [7]). When the temperature decreases: the viscosity and elasticity of the phases increase. It is well known that the coalescence rate can be reduced if the matrix becomes highly viscous [29,30]. For immiscible newtonian fluids and polymer blends, the coalescence efficiency increases (and the coalescence time decreases) as the viscosity of the

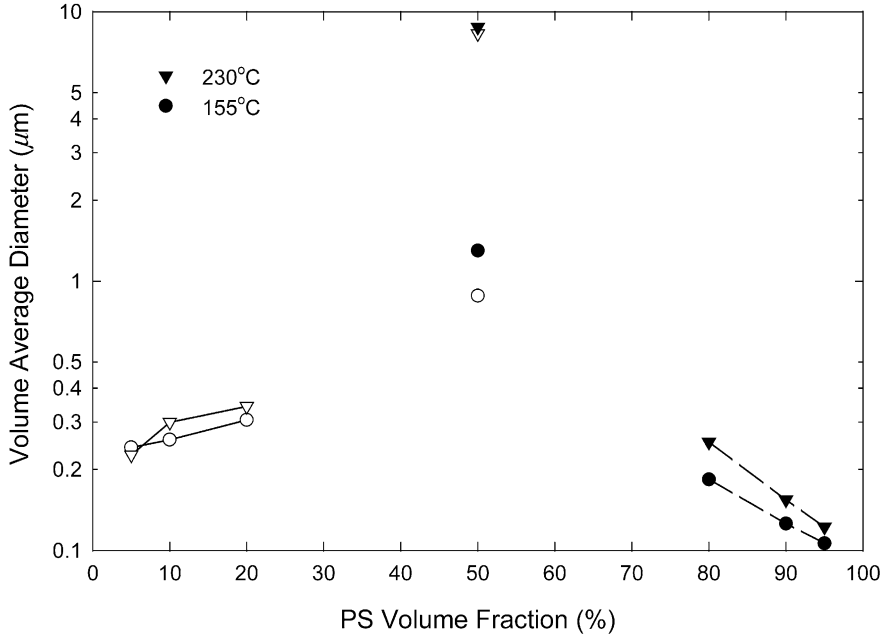

Fig. 4. Average diameters of dispersed phase for PCL/PS blends, as measured by image analysis and mercury intrusion porosimetry. White symbols denote the diameter after PS extraction, while black symbols denote the diameter after PCL extraction.

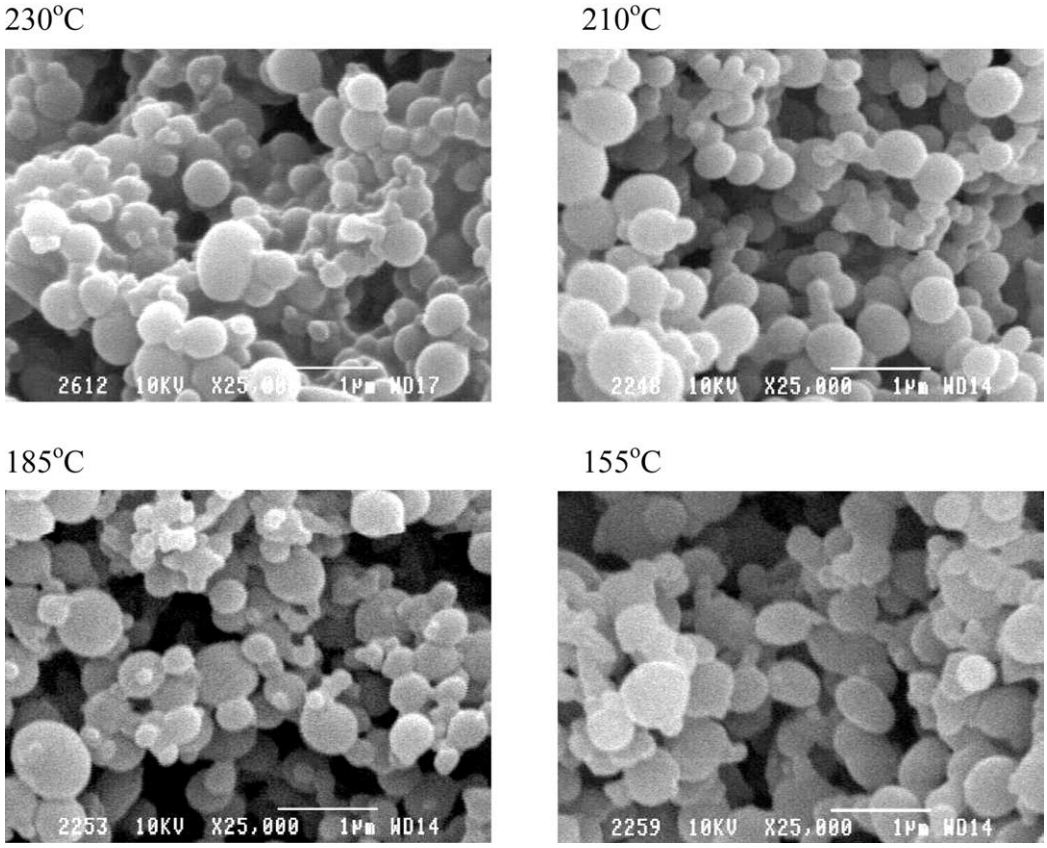

Fig. 5. PS dispersed phase obtained after matrix dissolution for the blends with 5%PS. The white bar denotes 1 μm.

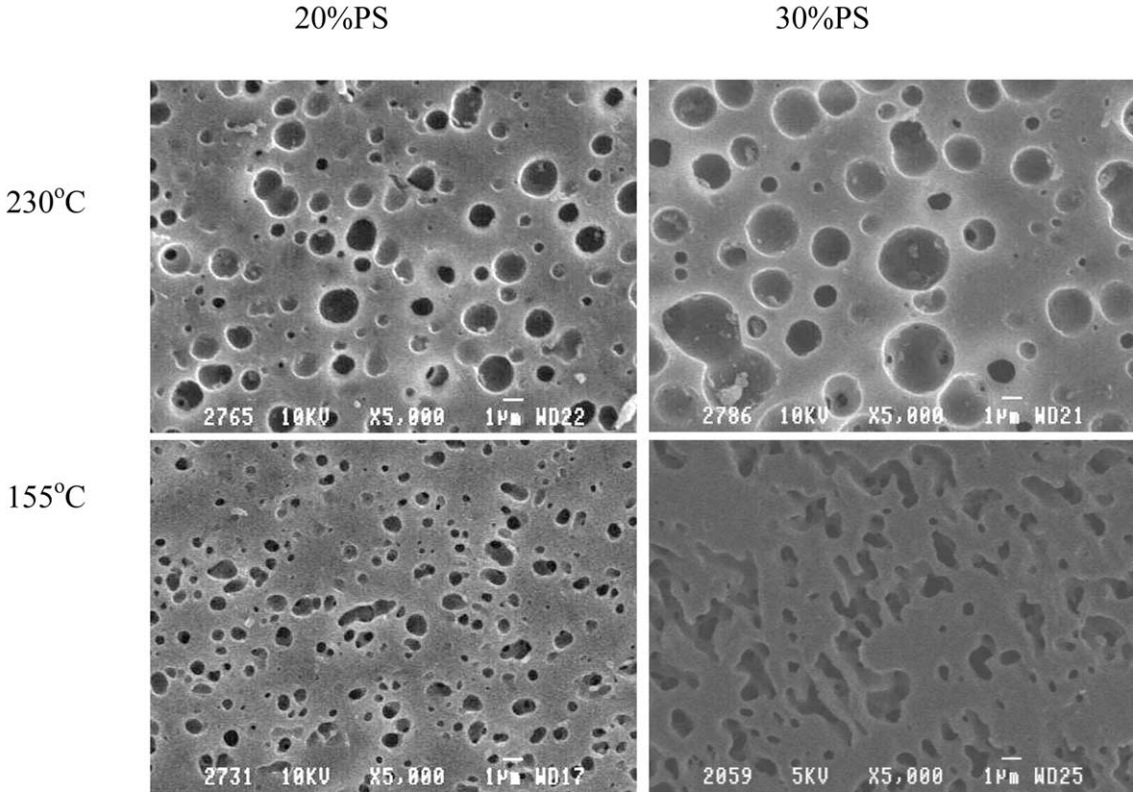

Fig. 6. SEM micrographs for PCL/PS 80/20 and 70/30 after the extraction of PS phase. The white bars indicate 1 μm.

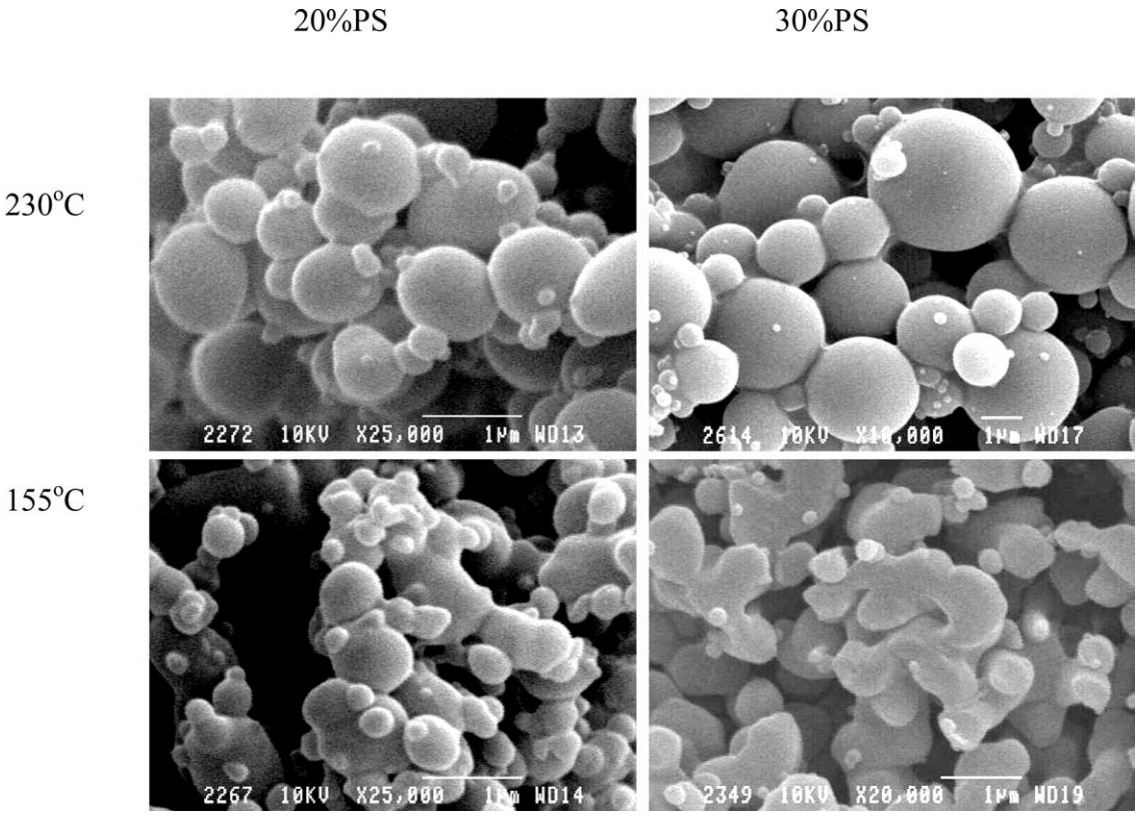

Fig. 7. PS dispersed phase obtained after matrix dissolution for the blends with 20 and 30%PS. The PS phase is found to be fully continuous in the blend PCL/PS 70/30 at 155 °C. The white bars indicate 1 μm.

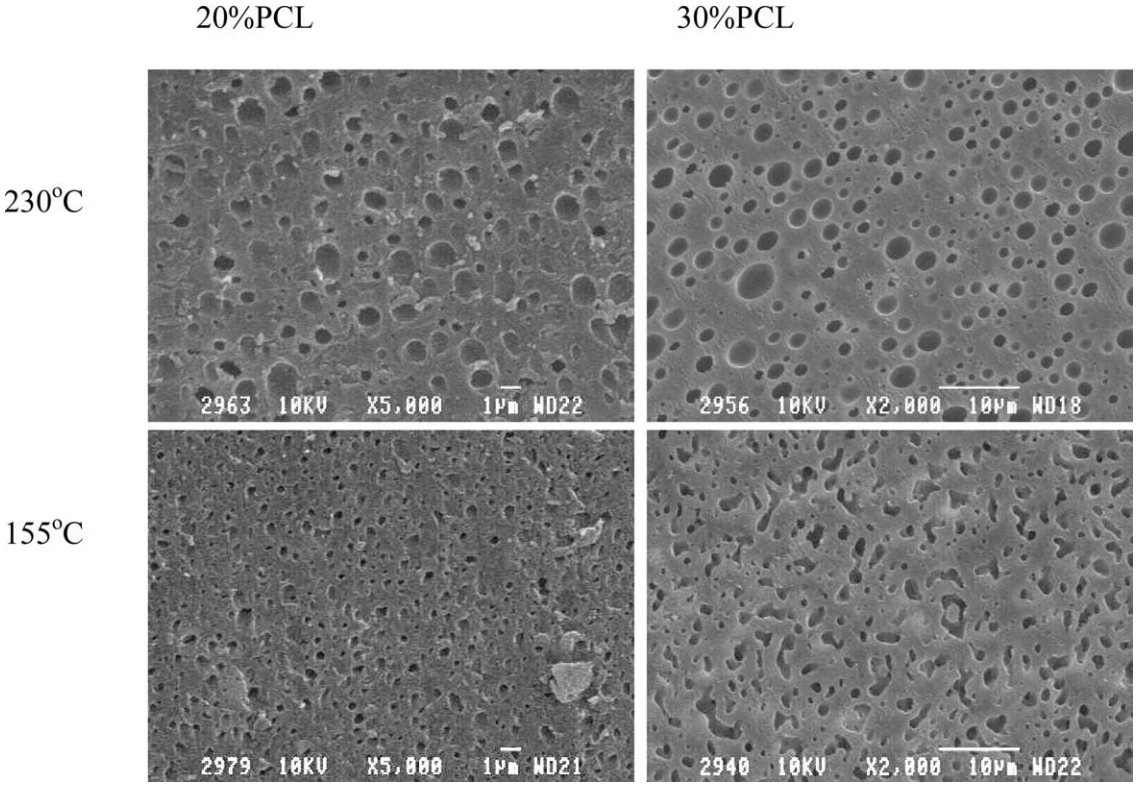

Fig. 8. SEM micrographs for PCL/PS 20/80 and 30/70 after the extraction of PCL phase. The white bars indicate 1 or 10 μm for the micrographs at 20 or 30% of dispersed phase, respectively.

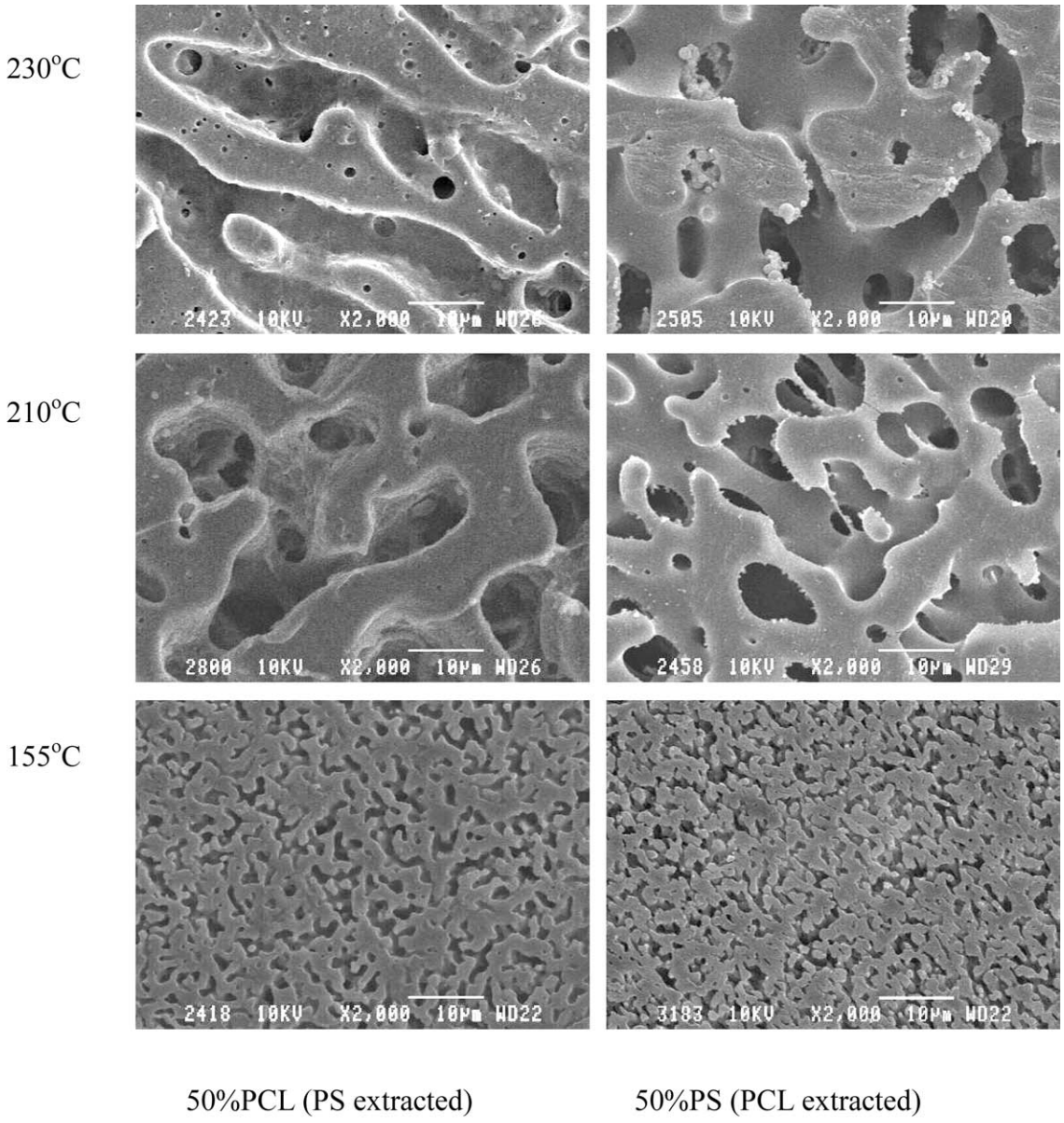

Fig. 9. SEM micrographs for PCL/PS 50/50 after the extraction of PS or PCL phase. The white bars indicate 10 μm.

matrix decreases [31–34]. Work has also been published that indicates that coalescence is greatly favored by low dispersed-phase viscosity [8,35]. Fig. 1 indicates that the viscosity of PS varies much more with temperature than the viscosity of PCL. When the temperature of mixing is reduced, it is especially the viscosity of PS that increases, meaning that the viscosity of the dispersed phase increases particularly in the PS in PCL matrix blends. It is this large increase in the dispersed phase viscosity which results in the incomplete merging of the dispersed droplet during coalescence. The asymmetric effect of temperature of mixing on the breadth of the region of dual-phase continuity (Fig. 10) can be explained since the effect of temperature on the viscosity of PCL is significantly less than the effect of temperature on the viscosity of PS. The retardation of the merging process is thus significantly less for dispersed PCL than for dispersed PS.

The coalescence mechanism for two spherical particles can be decomposed into four distinct stages: the collision between the two particles, the drainage of the matrix film separating the colliding particles, the rupture of the matrix film and the final merging into a fully coalesced larger spherical particle. If the particles enter in collision, the particles come closer and closer due to the hydrodynamic forces, resulting in a flattening of their interface in the contact region. The interaction time, i.e. the duration of the collision can be approximated by $t_{int} \sim 1/\dot{\gamma}$. In this study the external shear rate is the same for all experiments. If $t_{int} \geq t_{drain}$, there is sufficient time to allow for drainage of the film between the dispersed phase domains. Describing

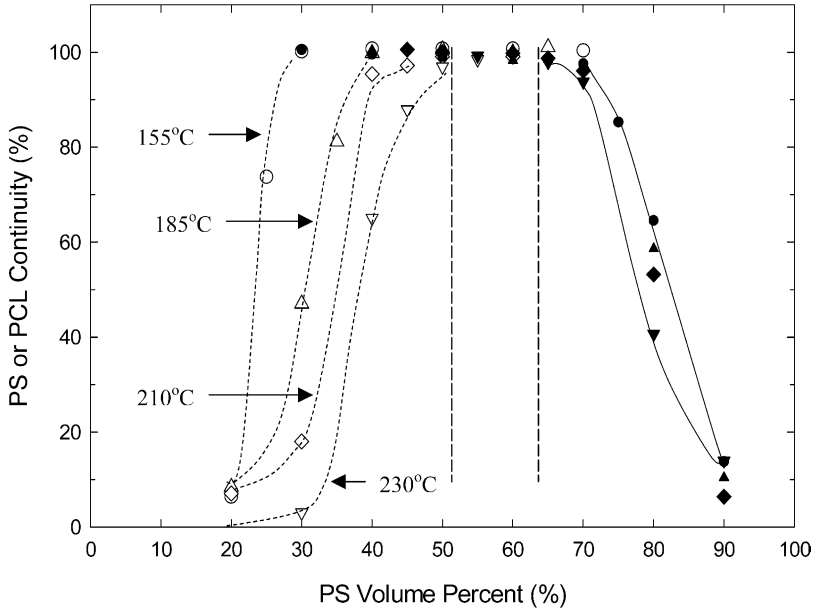

Fig. 10. Continuity of PS (dotted line) and PCL phase (solid line) as a function of the volume fraction of PS in the blends. The lines shown are presented as a guide for the eye.

the coalescence phenomena for two particles in a fluid, Chesters [8] points out that the models available for the coalescence deal with the sub-processes of collision, film drainage and film rupture. The drainage of the fluid is often considered to be the critical step in the coalescence process of two colliding droplets. Thus the area of confluence (i.e. the merging of the droplets after the film rupture) is generally omitted since once rupture has occurred so has coalescence, in the sense that a single connected domain of the dispersed phase has been created. Moreover, the first stage of confluence, the expansion of the hole in the film by interfacial tension will in fact be extremely rapid in view of the film's small thickness. About the later stage, Chesters states that it may take considerably longer and may, exceptionally, fail to reach completion due to disruptive forces exerted by the external flow. In the case of incomplete merging, the droplets are interconnected but the diameter of the particles is still not very changed. Thus the fusion of the particles, which corresponds to the real merging of the particles and results in the increase of the domain size, has not been significantly studied in the literature. In this work it is clearly the final merging process of coalescence that is the dominant factor in determining continuity development at low temperature for this PS-PCL system.

4. Conclusions

This paper demonstrates that temperature-induced coalescence effects during melt mixing have a major influence on the concentration range of dual-phase continuity and an order of magnitude effect on the co-continuous microstructure phase size. PCL and PS were blended in a batch mixer by only varying the mixing temperature. It is observed that the blending temperature has only a small effect on the morphology up to a PS or PCL composition of about 20%. However, at 20% and beyond that composition the effect is dramatic, due to flow driven coalescence. The microstructure of the 50/50 blend demonstrates a phase size (d_v) of 8.5 μm at 230 °C and 1.1 μm at 155 °C. The range of co-continuous structures can be extended from 50–65%PS at 230 °C to 30–70%PS at 155 °C. The effect of temperature on the concentration range of co-continuity and phase size is attributed to the incomplete merging of the dispersed phase during the coalescence phenomena at low temperature. This is a result of the very high increase of the viscosity of the dispersed phase when the mixing temperature is low. The effect of temperature on the viscosity of PS is much greater than that for PCL which leads to much more pronounced morphology effects for PS in PCL than for PCL in PS. This results in an asymmetric effect on the shift in the range of dual-phase continuity. These results underline that continuity models should include parameters related to coalescence effects as well as the absolute viscosities. The data indicate the significant potential of mixing temperature as a tool for the morphology control of co-continuous polymer blends, a parameter which has been mostly overlooked up to now.

Acknowledgements

The authors are grateful to the Natural Sciences and Engineering Research Council of Canada (NSERC) for funding this research through a strategic grant. P. Sarazin

expresses appreciation to the Province of Quebec for a postgraduate scholarship (Fonds Nature et Technologies, FCAR). The authors also thank Dr Johanne Denault and Ghislain Chouinard from IMI-NRCC for their help in measuring the polymer densities by PVT dilatometry.

References

[1] Favis BD. Factors influencing the morphology of immiscible polymer blends in melt processing. In: Paul DR, Bucknall CB, editors. Polymer blends volume 1: formulation. New York: Wiley; 2000. p. 501–38.
[2] Willemse RC, Posthuma de Boer A, van Dam J, Gotsis AD. Polymer 1999;40:827–34.
[3] Pötschke P, Paul DR. J Macromol Sci 2003;C43:87–141.
[4] Gubbels F, Blacher S, Vanlathem E, Jérôme R, Deltour R, Brouers F, et al. Macromolecules 1995;28:1559–66.
[5] Willemse RC, Speijer A, Langeraar AE, Posthuma de Boer A. Polymer 1999;40:6645–50.
[6] Sarazin P, Favis BD. Biomacromolecules 2003;4:1669–79.
[7] Li J, Ma PL, Favis BD. Macromolecules 2002;35:2005–16.
[8] Chesters AK. Trans IchemE 1991;69:259–70.
[9] Janssen JMH, Meijer HEH. Polym Eng Sci 1995;35:1766–80.
[10] Vinckier I, Moldenaers P, Terracciano AM, Grizzuti N. AIChE J 1998;44:951–8.
[11] Lyu SP, Bates FS, Macosko CW. AIChE J 2000;46:229–38.
[12] Lyu SP, Bates FS, Macosko CW. AIChE J 2002;48:7–14.
[13] Serpe G, Jarrin J, Dawans F. Polym Eng Sci 1990;30:553–65.
[14] Chaudhry BI, Hage E, Pessan LA. J Appl Polym Sci 1998;67: 1605–13.
[15] Lee JK, Han CD. Polymer 1999;40:6277–96.
[16] Bousmina M, Ait-Kadi A, Faisant JB. J Rheol 1999;43:415–33.
[17] Guo HF, Packirisamy S, Mani RS, Aronson CL, Gvozdic NV, Meier DJ. Polymer 1998;39:2495–505.
[18] Chen TH, Su AC. Polymer 1993;34:4826–31.
[19] Saltikov SA. In: Elias H, editor. Proceedings of the second international congress for stereology. Berlin: Springer-Verlag; 1967. p. 163–73.
[20] Washburn EW. Proc Natl Acad Sci 1921;7:115–6.
[21] Ritter HL, Drake LC. Ind Eng Chem 1945;17:782–6.
[22] Cox WP, Merz EH. J Polym Sci 1958;28:619–22.
[23] Laun HM. J Rheol 1986;30:459–501.
[24] Biresaw G, Carriere CJ. J Appl Polym Sci 2002;83:3145–51.
[25] Kamal MR, Lai-Fook R, Demarquette NR. Polym Eng Sci 1994;34: 1834–9.
[26] Chapleau N, Favis BD, Carreau PJ. Polymer 2000;41:6695–8.
[27] Ghodgaonkar PG, Sundararaj U. Polym Eng Sci 1996;(36):1656–65.
[28] Willemse RC, Posthuma de Boer JvD, Gotsis AD. Polymer 1999;40: 827–34.
[29] Sundararaj U, Macosko CW. Macromolecules 1995;28:2647–57.
[30] Fortelny I, Kovar J. Polym Compos 1988;9:119–24.
[31] Dreher TM, Glass J, O'Connor AJ, Stevens GW. AIChE J 1999;45: 1182–90.
[32] Mousa H, Agterof W, Mellema J. J Colloid Int Sci 2001;240:340–8.
[33] Wildes G, Keskkula H, Paul DR. Polymer 1999;40:5609–21.
[34] Roland CM, Bohm GGA. J Polym Sci, Polym Phys 1984;22:79–93.
[35] Schoolenberg GE, During F, Ingenbleek G. Polymer 1998;39:765–72.